OPEN ACCESS
Journal of Multidisciplinary Applied Natural Science Vol. xx No. xx (xxxx) https://doi.org/10.47352/jmans.2774-3047.353
Check for updates
Research Article

Enhanced Visible-Light Photocatalytic Degradation of Amoxicillin using TiO_2-Cu/N with Copper Sourced from Electroplating Wastewater

Kusuma Putri Suwondo, Endang Tri Wahyuni*, Nurul Hidayat Aprilita, Nur Farhana Jafaar, and Early Zahwa Alharissa

Received : November 27, 2025	Revised : December 23, 2025	Accepted : January 2, 2026	Online : January 23, 2026

Abstract
The growing prevalence of pharmaceutical contaminants, particularly amoxicillin (AMX), in aquatic environments poses serious threats to both ecosystems and public health. Addressing this issue requires the development of efficient photocatalysts capable of degrading such pollutants under visible-light irradiation. This study explores the enhanced photocatalytic degradation of AMX under visible light using copper and nitrogen co-doped titanium dioxide (TiO_2-Cu/N) synthesized utilizing copper recovered from electroplating wastewater. Comprehensive characterization through XRD, UV-Visible DRS, and TEM demonstrated that a Cu doping level of 0.60%, combined with 30% nitrogen co-doping and calcination at 500 °C, resulted in the most significant enhancement in photocatalytic activity under visible-light irradiation, attributed to the most effective bandgap narrowing. Notably, the TiO_2-Cu/N photocatalyst with optimized composition exhibited superior physicochemical properties and photocatalytic performance compared to its singly doped counterparts. The optimal condition of the AMX degradation was achieved using 100 mg of TiO_2-Cu/N to treat 100 mL of a 20 mg/L AMX solution at pH 6 under 2 h of visible-light irradiation, which was 90%. Furthermore, the Cu dopant in the TiO_2-Cu/N matrix remained stable during the photocatalytic process, as evidenced by the sustained activity even after three consecutive cycles. Additionally, the use of radical scavengers confirmed that hydroxyl radicals (•OH) were the predominant reactive species responsible for the degradation of amoxicillin. These findings highlight the promising potential of utilizing industrial wastewater as a dopant source for the sustainable development of high-performance photocatalysts in water treatment applications.

Keywords: amoxicillin, Cu-N, double dopant, photocatalysis, TiO_2, visible light, wastewater reuse

1. INTRODUCTION

The extensive use of antibiotics during the COVID-19 pandemic, which began in 2019, was widely reported, primarily as a preventive measure against secondary bacterial infections associated with the virus [1]. Among the most frequently administered antibiotics was amoxicillin (AMX), favoured for its rapid absorption in the human body [2]-[5]. Owing to its relatively slow metabolic rate, approximately 85% of administered AMX is excreted unchanged through urine and fecal matter [2]-[7]. These residues are subsequently discharged into wastewater systems and ultimately released into the environment. Additional sources of AMX contamination in aquatic ecosystems include hospital effluents, veterinary clinics, and pharmaceutical manufacturing facilities [3]-[5].

The AMX's chemically stable structure, as illustrated as Figure 1, renders it resistant to natural biodegradation [3]-[6], leading to its accumulation in water bodies. This persistence poses toxicological risks to aquatic organisms such as algae and plankton, potentially disrupting ecosystems and contributing to chronic health issues in humans [1]-[7]. Given these environmental and public health concerns, effective treatment strategies are urgently needed to mitigate AMX contamination. One promising approach is photocatalytic degradation [2]-[5][7], particularly using UV light in conjunction with titanium dioxide (TiO_2) photocatalyst.

Photodegradation involves the generation of reactive oxygen species, such as hole (h^+), as well as hydroxyl (•OH) and superoxide ($•O_2^-$) radicals, when TiO_2 is irradiated with UV light. The key reactions are as follows Equations (1) – (5) [2][3] [5][8]-[29]:

$$TiO_2 + hv \rightarrow TiO_2\ (e^- + h^+) \quad (1)$$
$$TiOH + h^+ \rightarrow Ti–•OH \quad (2)$$
$$h^+ + H_2O \rightarrow •OH + H^+ \quad (3)$$
$$e^- + O_2 \rightarrow •O_2^- \quad (4)$$

Publisher's Note:
Pandawa Institute stays neutral with regard to jurisdictional claims in published maps and institutional affiliations.

Copyright:
© 2026 by the author(s).
Licensee Pandawa Institute, Metro, Indonesia. This article is an open access article distributed under the terms and conditions of the Creative Commons Attribution (CC BY) license (https://creativecommons.org/licenses/by/4.0/).

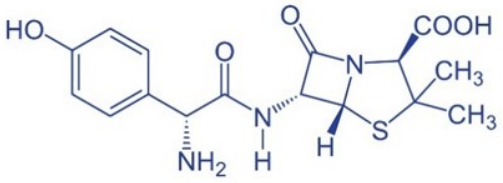

Figure 1. The chemical structure of AMX [3].

Table 1. Volume variation of solution B as the prepared solution of electroplating wastewater for Cu source for TiO_2 photocatalyst doping.

Volume of solution A (mL)	Volume of solution B (mL)	Calculated mg Cu/g TiO_2	Calculated Cu in TiO_2 (%w)
10	2.1	2	0.24
10	8.4	8	0.60
10	12.6	12	0.96

$TiO_2 + e^- + h^+ \rightarrow TiO_2 + heat$ **(5)**

These radicals are highly reactive and capable of degrading even structurally stable organic pollutants [2]-[3][8]-[12].

TiO_2 is widely used due to its chemical stability, low cost, and environmental safety [2][3][5][7]-[30]. However, its wide band gap energy (Eg = 3.2 eV) restricts its photocatalytic activity to the UV spectrum, which comprises only about 4% of sunlight [4][5][14]-[29]. This limitation hinders its effectiveness under natural sunlight and contributes to inefficient electron excitation and recombination, reducing overall photocatalytic performance [9]-[23]. Since visible light accounts for approximately 50–60% of solar radiation [4][7][15]-[17][19][23], considerable efforts have been made to modify TiO_2 for enhanced activity under visible light. Doping with non-metal [13]-[17] and metal atoms [18]-[22] has proven effective in narrowing the band gap and suppressing electron-hole recombination, thereby improving photocatalytic efficiency [13]-[22].

Copper (Cu), a transition metal, is a promising dopant due to its atomic size compatibility with titanium. Cu doping introduces 3d orbitals below the conduction band, reducing the band gap and facilitating electron capture to inhibit recombination [19]-[22]. Nitrogen (N), a non-metal dopant, also enhances TiO_2 performance due to its atomic size similarity with oxygen. N atoms can substitute or bond with O or Ti atoms, forming 2p orbitals above the valence band and further narrowing the band gap [13][15]-[17]. Single-element doping often requires high dopant concentrations, which may introduce recombination centres and reduce photocatalytic activity [20][23]-[27]. To address this weakness, dual-doping strategies of non-metal + non-metal [23][24], metal + metal [25][26], and non-metal + metal [26][27][29] have been explored. Among these, non-metal + metal combinations are considered the most effective, as the presence of larger metal atoms facilitates non-metal incorporation.

Recent studies have demonstrated that doping TiO_2 with a single dopant of Cu and nitrogen N significantly enhances its photocatalytic activity under visible light [26][27][29]. Urea is widely used as a cost-effective nitrogen source [13][15]-[17][23][24][26][27], while Cu is typically introduced through commercial salts [18]-[22], which are relatively expensive. Interestingly, copper can also be recovered from electroplating wastewater, which contains high concentrations of Cu and poses environmental risks. In our previous research [29], we successfully synthesized N co-doped Cu-TiO_2 using copper derived from electroplating wastewater. However, that study did not investigate the photocatalytic activity of TiO_2-Cu with varying Cu concentrations for the degradation of AMX under visible light irradiation. Moreover,

optimization of the calcination temperature during the synthesis of N co-doped TiO_2-Cu, which could yield the lowest bandgap energy and highest photocatalytic performance, was not conducted. Further optimization of various process parameters also remains unexplored.

In light of these considerations, in the present study photocatalytic degradation efficiency of AMX using TiO_2 co-doped with nitrogen and copper, sourced from electroplating wastewater, was systematically evaluated under visible-light irradiation. The effects of varying dopant concentrations and calcination temperatures on the performance of the TiO_2-Cu/N photocatalyst were thoroughly investigated. Additionally, key process parameters, including catalyst dosage, solution pH, and reaction time, were systematically optimized to enhance the degradation efficiency. Furthermore, the reactive species involved in the degradation mechanism were identified to gain deeper insight into the photocatalytic process.

2. MATERIALS AND METHODS

2.1. Materials

Titanium(IV) isopropoxide (TTIP, $C_{12}H_{28}O_4Ti$; 98%) was obtained from Shanghai Chemical Industry, while urea (CH_4N_2O), absolute ethanol (99.99%), nitric acid (65%), amoxicillin trihydrate ($C_{16}H_{25}N_3O_8S$), isopropanol (C_3H_8O, 98%), sodium hydroxide (NaOH), disodium ethylenediaminetetraacetate (Na_2EDTA, $C_{10}H_{14}N_2Na_2O_8 \cdot 2H_2O$), and analytical-grade ammonium oxalate were purchased from Merck. All chemicals were used without further purification. Electroplating wastewater was collected from an industrial facility located in the Yogyakarta region, Indonesia.

2.2. Methods

2.2.1. Analysis of the Electroplating Wastewater

The concentrations of copper (Cu) and other metal ions present in electroplating wastewater

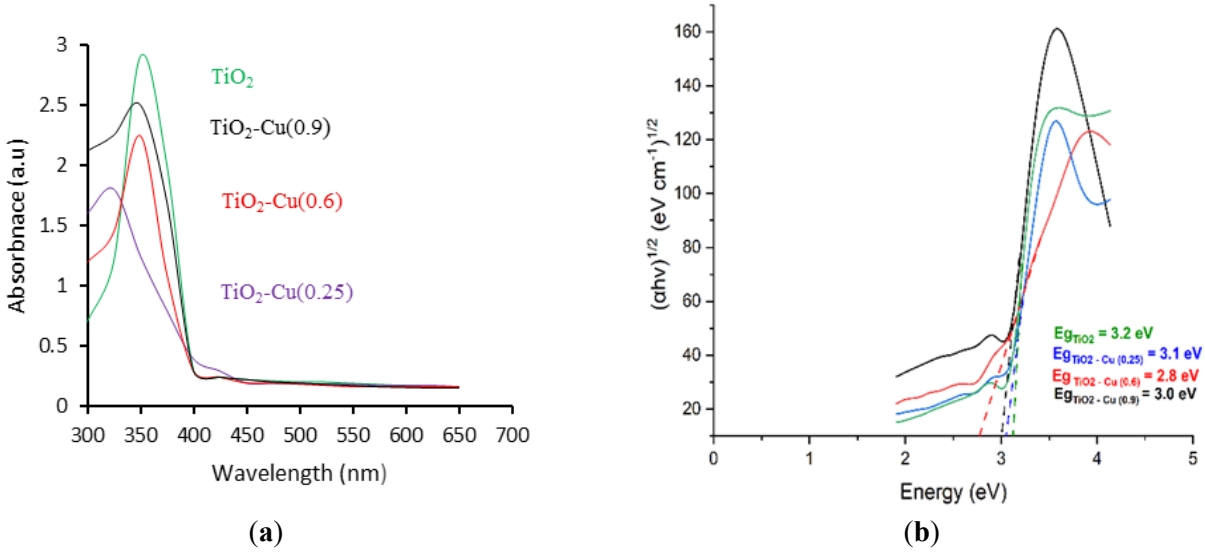

(**a**) (**b**)

Figure 2. The DR-UV/Vis spectra (a), and the Tauc plot (b) for TiO_2-Cu-photocatalysts with different Cu fractions.

Table 2. The effect of Cu dopant and its fraction on the Eg reduction.

Photocatalysts	λ (nm)	Eg (eV)
TiO_2	385.09	3.20
TiO_2−$Cu_{0.24}$	389.94	3.10
TiO_2−$Cu_{0.6}$	430.56	2.80
TiO_2−$Cu_{0.9}$	396.17	3.00

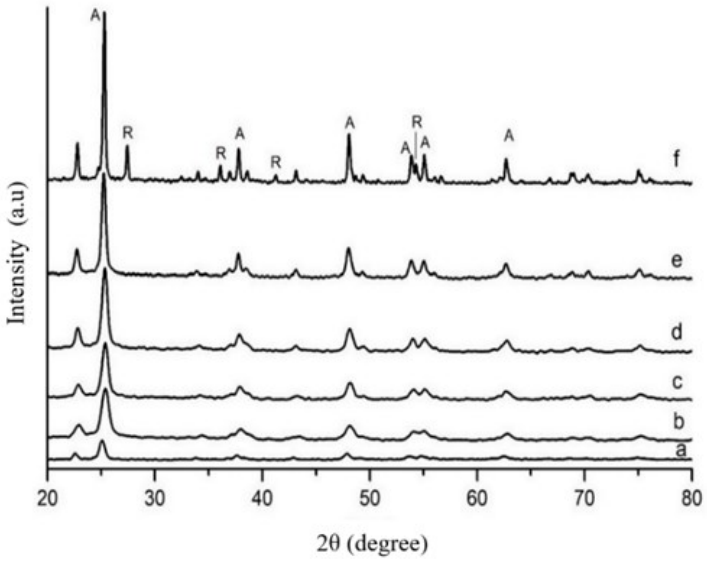

Figure 3. XRD patterns of TiO_2-Cu/N calcined at (a) 100; (b) 350; (c) 450; (d) 500; (e) 550; (f) 650 ^oC where "A" stands for anatase, and "R" stands for rutile as the main crystal phases in TiO_2.

Table 3. Effect of the synthesis calcination temperature of TiO_2-Cu/N on the crystal size.

Calcination temperature (°C)	Average crystal size (nm)
350	5.36
450	8.84
500	9.45
550	13.75
650	19.61

were determined using an atomic absorption spectrophotometer (AAS, Perkin Elmer 3110). Prior to analysis, the wastewater samples were acidified with concentrated nitric acid to adjust the pH to below 2. This step ensures complete dissolution of metal ions, allowing for accurate and reliable quantification.

2.2.2. Synthesis of Cu-doped TiO_2

The synthesis process began by adding 2 mL of Titanium Tetraisopropoxide (TTIP) into 10 mL of ethanol, followed by stirring at a moderate speed for 30 min. This mixture was designated as solution A. Cu-doped TiO_2 was then prepared via a sol–gel method. Specifically, 1 mL of electroplating wastewater which contains approximately 24,000 mg/L of copper, as determined by AAS. Other metal ions present in the wastewater included Zn (160 mg/L), Fe (3.550 mg/L), Ni (0.8 mg/L), Cd (0.4 mg/L), and Co (0.002 mg/L), confirming that copper was the dominant component. That wastewater sample was mixed with ethanol and diluted with distilled water to a final volume of 10 mL. The pH of the resulting solution was adjusted to 3 using 0.1 M HNO_3, and this mixture was labeled as solution B. To achieve varying Cu doping levels, different volumes of solution B were added dropwise into separate batches of solution A, as detailed in Table 1. The photocatalysts obtained were codes as TiO_2-$Cu_{0.24}$, TiO_2-$Cu_{0.6}$, and TiO_2-$Cu_{0.9}$ following the fraction of Cu in the doped TiO_2.

2.2.3. Synthesis of TiO_2-N Photocatalyst

The TiO_2-N photocatalyst was synthesized with a nitrogen content of 30%, corresponding to the previously reported optimal doping level. To achieve this, 11.4 mL of a urea solution (6 g/L), serving as the nitrogen source, was added to 10 mL of solution A. The mixture was stirred at 600 rpm for 1 h and then left to stand overnight at room

temperature to facilitate gel formation. The resulting gel was dried at 80 °C for 5 h, followed by calcination at 500 °C for 2 h. The final product was designated as TiO_2-N(30), reflecting the nitrogen fraction introduced based on the volume of urea solution used during synthesis.

2.2.4. Synthesis of TiO_2-Cu from Electroplating Wastewater Co-doped with Nitrogen

The synthesis procedure for the co-doped photocatalyst followed the same method as that used for TiO_2-Cu and TiO_2-N. In this case, 10 mL of solution A was combined with 11.4 mL of a urea solution (6000 mg/L) and 8.4 mL of electroplating wastewater containing 24,000 mg/L of copper. The resulting co-doped photocatalyst was designated as TiO_2-Cu/N (30:0.6), indicating the respective nitrogen and copper fractions introduced during the synthesis. Then, the mixture was stirred at 600 rpm for 1 h and then left to stand overnight at room temperature to facilitate gel formation. The resulting gel was dried at 80 °C for 5 h, followed by calcination at various temperatures of 350, 450, 500, 550, and 650 °C, respectively. This study and procedure aim to determine the optimal calcination temperature for synthesizing TiO_2-Cu co-doped with nitrogen.

2.2.5. Characterization

In this study, several characterization techniques were employed, including a diffuse reflectance UV-visible (DR-UV/Vis) spectrophotometer from Analytik Jena (SPECORD 200 plus) for measuring the concentration of AMX pollutant, X-ray diffraction (XRD) from Shimadzu 6000D to evaluate the crystallinity on the photocatalyst compound, and transmission electron microscopy (TEM) JEOL JEM-1400 to acquire the crystal size of photocatalyst material. For DR-UV/Vis analysis, fine photocatalyst powder was placed in a designated cuvette and measured across a wavelength range of 300–800 nm. XRD analysis

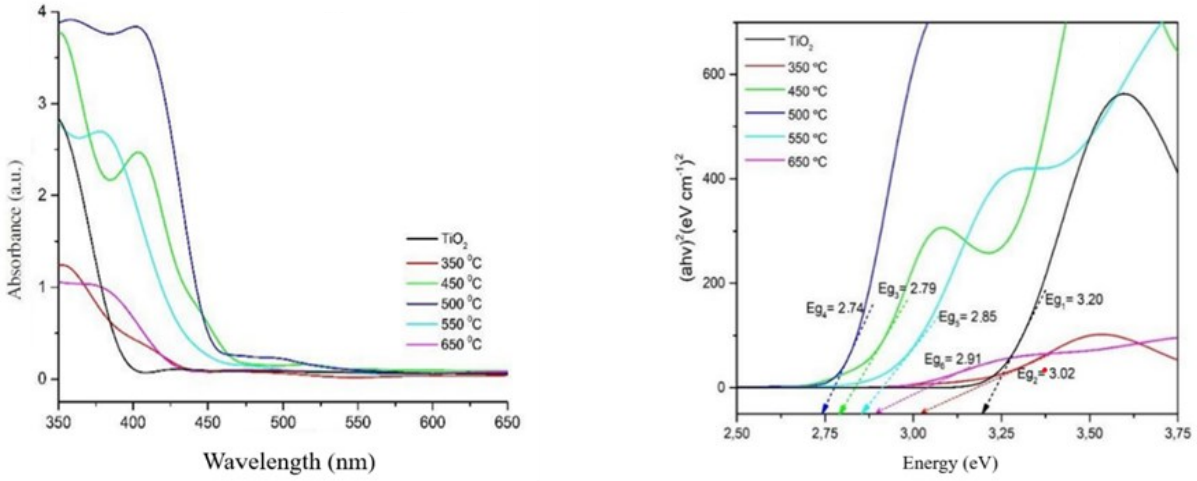

(a) **(b)**

Figure 4. The effect of the calcination temperature on (a) DR-UV/vis spectra, and (b) The Tauc plot results, of the TiO_2-Cu/N.

Table 4. The effect of the synthesis calcination temperature of TiO_2-Cu/N on the Eg values.

Photocatalysts	λ (nm)	Eg (eV)
TiO2	387.50	3.20
TiO2−Cu/N (350)	410.59	3.02
TiO2−Cu/N (450)	444.44	2.79
TiO2−Cu/N (500)	452.55	2.74
TiO2−Cu/N(550)	435.09	2.85
TiO2−Cu/N (650)	426.12	2.91

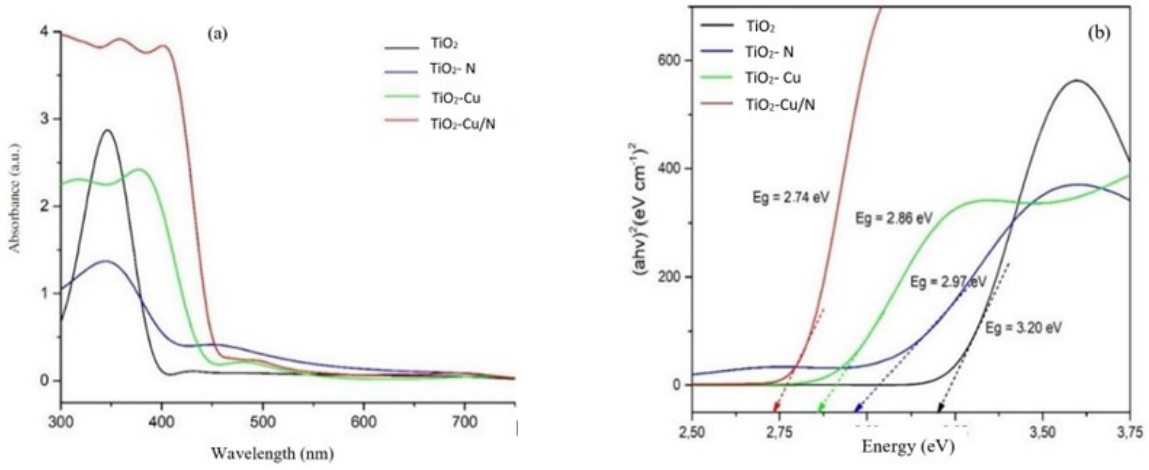

(a) **(b)**

Figure 5. Effect of N co-doped inti TiO_2-Cu on : (a) DR-UV/Vis. spectra, and (b) on the Tauc plot results.

Table 5. The effect of N-co-dopant on the Eg values of TiO_2-Cu/N.

Photocatalysts	λ (nm)	E_g (eV)
TiO_2	387.50	3.20
TiO_2–$N_{(30)}$	417.51	2.97
TiO_2–$Cu_{(0.6)}$	430.56	2.88
TiO_2–$Cu/N_{(500)}$	452.56	2.74

was conducted using an instrument equipped with a Cu-Kα radiation source (λ = 1.5406 Å), operated at 40 kV and 30 mA. The powder samples were uniformly spread onto a metal sample holder, and diffraction patterns were recorded over a 2θ range of 3–80°. The TEM observation was performed at an acceleration voltage of 120 kV, and the samples were dispersed in deionized water homogenously and dropped onto Cu grid.

2.2.6. Photodegradation Test of AMX

A 100 mL aqueous solution of AMX, with an initial concentration of 20 mg/L, was combined with 100 mg of TiO_2 photocatalyst, corresponding to a dosage of 1 g/L. The mixture was stirred continuously for 15 min in the dark to establish adsorption–desorption equilibrium. Following this pre-treatment, the suspension was exposed to irradiation for 1 h in a sealed chamber equipped with both UV and visible light sources. That UV box reactor is equipped with UVA lamps (4×18W, 320-400 nm) and LED lamps (4×20 watt, Philips). After irradiation, the suspension was centrifuged at 1000 rpm for 10 min to separate the solid photocatalyst from the liquid phase. The resulting clear supernatant was collected, and its absorbance was measured at 280 nm using a UV-vis spectrophotometer, which corresponds to the maximum absorbance wavelength of AMX. The absorbance values were then interpolated against a standard calibration curve to determine the residual concentration of undegraded AMX.

This procedure was repeated for various photocatalysts, including TiO_2-Cu with different Cu loadings, TiO_2-N, and TiO_2-Cu/N with the optimal dopant ratio and at various calcination temperatures. Additional experiments were carried out to investigate the effects of reaction time, photocatalyst dosage, and solution pH on the degradation efficiency. Moreover, radical scavenger tests were conducted using ammonium oxalate ($(NH_4)_2C_2O_4$), isopropanol, and Na_2EDTA to identify the reactive species involved in the photocatalytic degradation process. All experiments for determining the optimal photodegradation condition were conducted three times.

3. RESULTS AND DISCUSSIONS

3.1. Characterization

3.1.1. Effect of Cu-doping at Various Concentrations on the Eg of TiO_2

Prior to conducting nitrogen co-doping on Cu-doped TiO_2 photocatalysts, Cu doping was first performed on TiO_2 using a range of Cu concentrations to determine the optimal Cu content. This is defined as the amount of Cu that maximally declines the band gap energy (Eg) of TiO_2. The Eg values of both pristine and Cu-doped TiO_2 were determined from DRUV spectra by using the Tauc plot, as illustrated in Figure 2.

The obtained data indicate that Cu doping effectively lowers the band gap energy (Eg) by narrowing the semiconductor structure of TiO_2 (Table 2). Moreover, increasing the concentration of Cu dopants further enhances this band gap narrowing effect. However, when the dopant level becomes excessively high, the narrowing effect begins to diminish. This reduction in band gap is attributed to the contribution of electrons in the d-orbitals of Cu atoms, which overlap with the d-orbitals of Ti atoms, leading to band broadening just below the conduction band [18]-[22][28]. As the Cu concentration increases, this band broadening becomes more pronounced. Nevertheless, excessive Cu doping impedes its incorporation into the TiO_2 lattice, thereby reducing its contribution to band broadening. The resulting decrease in Eg values after doping shifts the absorption into the visible light region, offering potential for enhanced photocatalytic activity under visible light irradiation. Based on the obtained Eg data, it is confirmed that the optimal Cu concentration for effectively decreasing the band gap in TiO_2-Cu is 0.60%, which will be used in the subsequent experimental stages.

3.1.2. Effect of Co-doping N on the Character of TiO_2-Cu/N

During the co-doping process to form TiO_2-Cu/N, calcination was carried out at various temperatures, and its effect on crystal growth was examined based on the XRD patterns shown in Figure 3. These patterns demonstrate an increase in the crystallinity of the photocatalyst as the calcination temperature rises to 550 °C. At a higher temperature of 650 °C, crystallinity continues to improve. However, partial phase transformation from anatase to rutile is also observed, while the anatase phase remains detectable. Previous studies have reported that this phase transition typically begins around 600 °C and requires temperatures up to 700 °C for complete conversion [30][31]. These findings suggest that the presence of dual dopants (N and Cu) delays the phase transformation, indicating that the dopants help stabilize the anatase crystal structure at elevated temperatures.

The impact of calcination temperature on the average crystallite size of the TiO_2-Cu/N is summarized in Table 3. An increase in calcination temperature corresponds with a growth in crystallite size. Elevated temperatures provide sufficient energy for atoms to migrate and rearrange, allowing smaller crystallites to merge into larger ones. This coalescence reduces grain boundaries and increases the average crystal size. Higher calcination temperatures also help eliminate structural defects and disordered regions, encouraging the formation

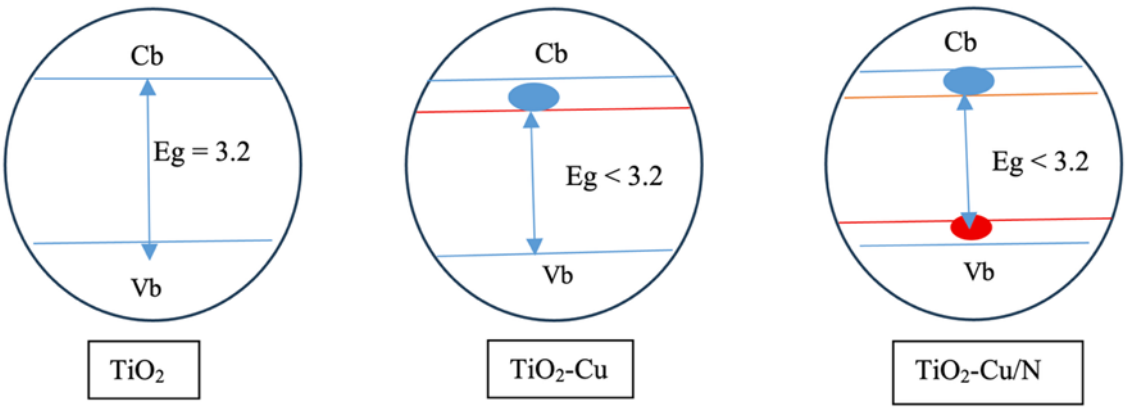

Figure 6. Illustration of band gap energy (Eg) in undoped, doped, and co-doped TiO_2.

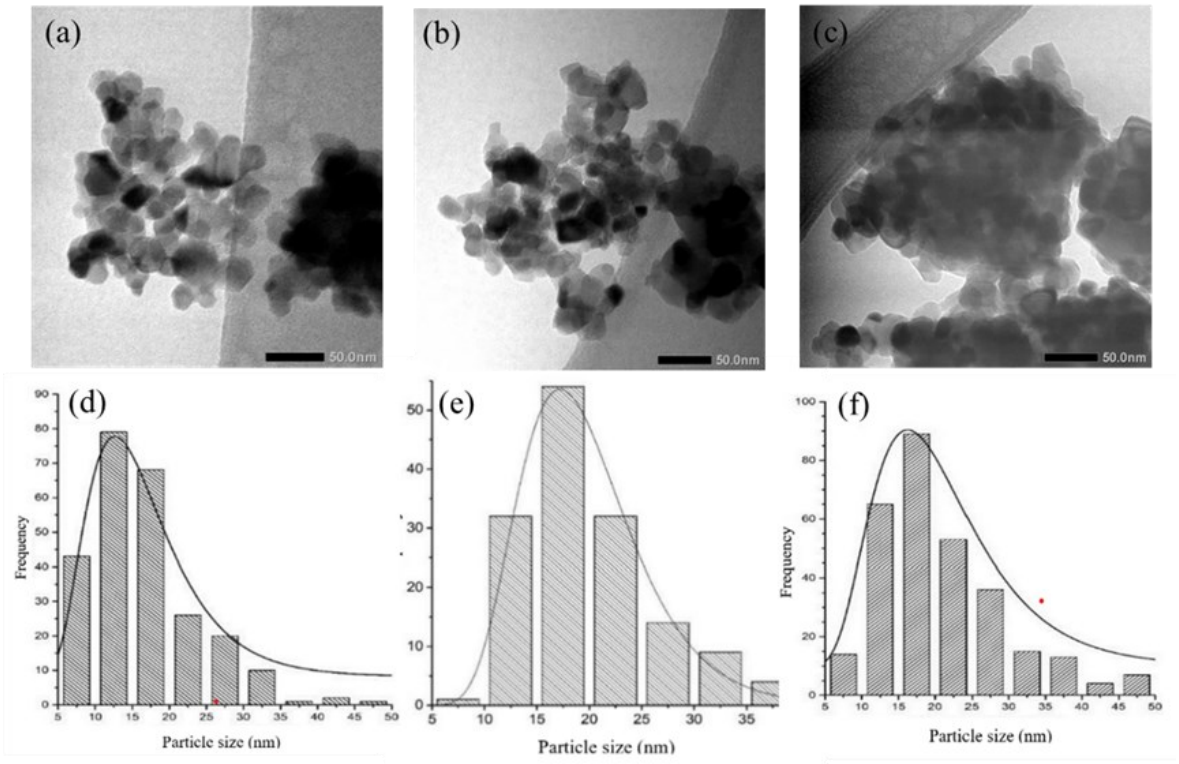

Figure 7. The TEM images and representative of its particle size chart distribution, respectively for (a,d) TiO_2, (b,e) TiO_2-$Cu_{(0.6)}$, and (c,f) TiO_2- $Cu/N_{(500)}$ to observe the effect of single Cu and dual N–Cu doping on the morphology and the particle size distribution of the modified TiO_2 photocatalysts.

of well-ordered crystalline domains [30]. As the temperature increases to 650 °C, the system tends to favour thermodynamically stable phases with larger crystal sizes, such as rutile, which typically forms at higher temperatures and exhibits larger grains than anatase.

Furthermore, the effect of calcination temperature on the light absorption capability and Eg values of TiO_2-Cu/N was also evaluated. The corresponding absorption spectra are presented in Figure 4, while the Eg values, determined using the Tauc Plot method, are summarized in Table 4. The data in the Table reveal a clear trend in which increasing the calcination temperature during the TiO_2-Cu/N synthesis leads to a reduction in the Eg. This behaviour is attributed to improved dopant incorporation and lattice ordering at elevated temperatures, which facilitate the formation of defect states that contribute to band gap narrowing and better charge carrier mobility [30]. However, when the calcination temperature becomes excessively high, a partial phase transformation from anatase to rutile occurs, and the effectiveness of band gap narrowing diminishes. As a result, the decrease in Eg becomes less significant at higher temperatures, indicating a trade-off between crystallinity improvement and phase stability [31]. Based on the effectiveness of Eg reducing lowering, it is clear that the best calcination temperature refers to 500 °C.

To address the objectives of this study, a comparative analysis was conducted between the effect of dual doping with Cu and N and the individual effects of single doping with either Cu or N on the reduction of Eg. The DR-UV/vis spectra and corresponding Tauc plots of these materials are presented in Figure 5, while the calculated Eg values are summarized in Table 5. Figure 5 and Table 5 reveal that dual doping effectively shifts the absorption edge into the visible light region and results in a more substantial band gap narrowing compared to single-element doping. The narrowing effect of Cu doping is associated with the introduction or broadening of energy states below the conduction band, as previously discussed. In contrast, nitrogen doping contributes to band gap reduction through the interaction between nitrogen's p-orbital electrons and those of oxygen,

leading to the formation of new energy states above the valence band. Thus, it is evident that the more pronounced band gap narrowing observed with dual doping arises from the synergistic effect of band broadening both below the conduction band (Cb) and above the valence band (Vb), as depicted in Figure 6.

To further support the XRD data regarding the effect of Cu doping as well as N/Cu co-doping on the particle size of TiO_2 photocatalysts, TEM images were obtained. As shown in Figure 7, TEM images of TiO_2 show spherical and irregular-shaped nanoparticles and they are aggregated. This could be due to the rapid hydrolysis of TTIP catalyzed by diluted HNO_3.

In TEM images of Cu-doped TiO_2, copper appears as small dark spots, either dispersed across the surface or embedded within the TiO_2 particles. Copper doping also induces morphological changes, leading to more irregular particle shapes. Moreover, the images show that Cu incorporation increases the primary particle size distribution to approximately 15–20 nm, compared to undoped TiO_2, which predominantly exhibits particle sizes in the range of 10–15 nm. Copper ions may act as facilitators during thermal treatment by enhancing atomic mobility and promoting grain coalescence [18][19] [21][22]. Additionally, the substitution of Cu^{2+} into the TiO_2 lattice can introduce local lattice distortions that favor crystal growth over nucleation, ultimately resulting in larger particle formation [21][22].

In the Cu-N co-doped TiO_2 photocatalyst, the TEM images display that the dark spots corresponding to Cu dopant are not clearly visible, possibly due to being covered by a thin layer, which may consist of nitrogen. Moreover, nitrogen co-doping appears to have minimal impact on the particle size distribution, with the majority of particles consistently measuring between 15 and 20 nm. This suggests that nitrogen typically substitutes for oxygen or occupies interstitial sites without significantly altering the crystal growth kinetics [26][27]. Further, the presence of nitrogen may counterbalance the growth-promoting effect of copper, possibly by introducing defect states or limiting atomic diffusion during calcination [26] [27].

3.2. Activity Assessment of TiO_2 Effected by Single and Dual Dopants

3.2.1. The Effect of Single Dopant Cu Dopant Fraction

The photodegradation performances of AMX using TiO_2 photocatalysts doped with Cu with varying copper concentrations are illustrated in Figure 8 (panels 1–4). Overall, it is evident that Cu doping enhances the photodegradation efficiency, with further improvements observed as the Cu content increases. However, an excessive amount of Cu leads to a decline in performance. This trend aligns with the corresponding Eg values. The presence of Cu dopant enhances visible light

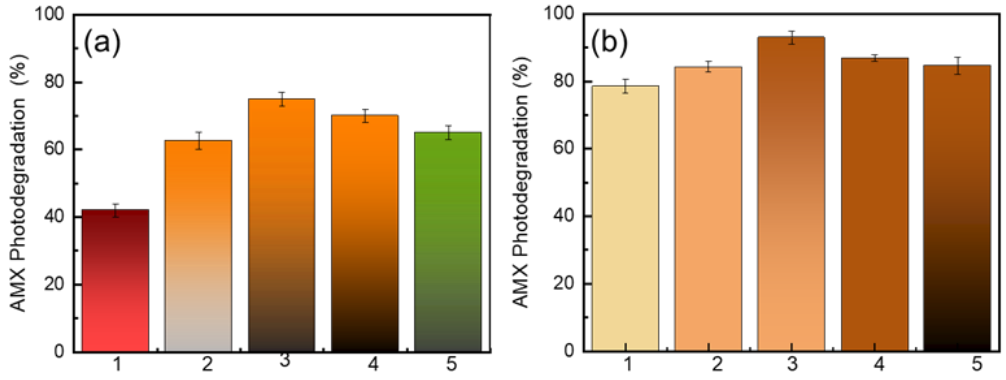

Figure 8.(a) the AMX photodegradation over : 1)TiO_2, 2) TiO_2-$Cu_{(0.25)}$ 3) TiO_2-$Cu_{(0.60)}$ 4) TiO_2-$Cu_{(0.90)}$, and 5) TiO_2-$N_{(30)}$, and (b) 1) TiO_2-Cu/$N_{(350)}$, 2) TiO_2-Cu/$N_{(450)}$, 3) TiO_2-Cu/$N_{(500)}$, 4) TiO_2-Cu/$N_{(550)}$ and 5) TiO_2-Cu/$N_{(650)}$ corresponding to the effect of Cu doping ratio and calcination temperatures for synthesizing the co-doping photocatalyst.

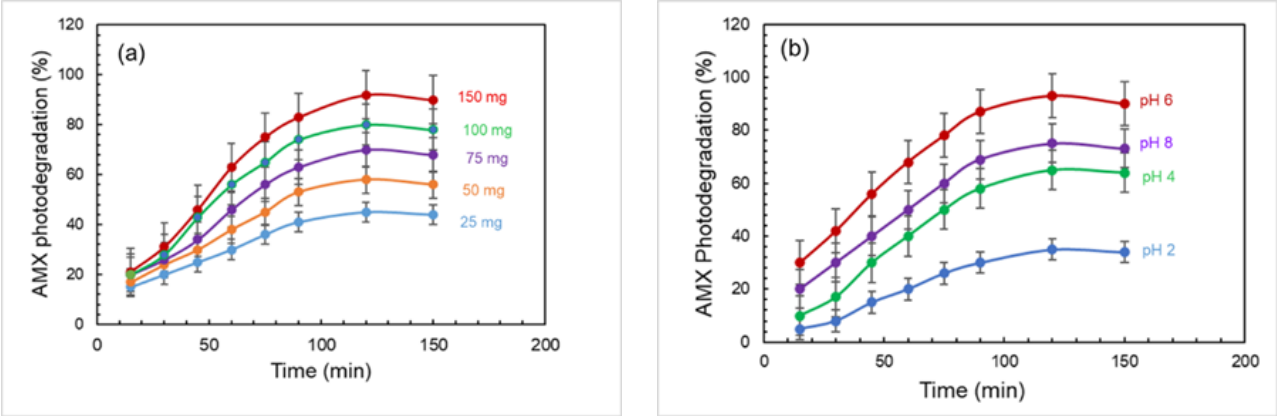

Figure 9. The effects of reaction time on (a) photocatalyst mass, and (b) solution pH, on the photodegradation efficiency.

absorption, thereby generating more •OH radicals that contribute to the degradation of AMX. Additionally, as a transition metal, Cu provides vacant d orbitals that can trap electrons from the conduction band. This process helps suppress electron-hole recombination, allowing more •OH radicals to form. However, at higher concentrations of Cu, light absorption tends to decrease, leading to a reduced generation of •OH radicals. In addition, an excessive amount of Cu may coat the surface of the photocatalyst, thereby obstructing the interaction between AMX molecules and the active •OH radicals. Based on the observed results, the optimal Cu doping level is identified to be 0.60 %, which is recommended for further investigation.

3.2.2. The Effect of Optimization Co-doping N and Its Calcination Temperature

Figure 8(a) provides further insight into the impact of nitrogen co-doping on the photocatalytic activity of TiO_2–Cu/N synthesized at different temperatures. The findings clearly indicate that nitrogen incorporation significantly enhances the performance of TiO_2–Cu/N under visible light irradiation, surpassing the activity achieved through individual doping with either Cu or N alone. This trend can be attributed to the more effectively reduced band gap energy (Eg) of the TiO_2-Cu/N photocatalyst compared to its singly doped counterparts, resulting in significantly enhanced absorption of visible light. The enhanced light-harvesting capability facilitates the generation of a higher level of •OH radicals, which are essential for the degradation of organic pollutants.

Moreover, Cu doping plays a critical role by acting as an electron trap, effectively suppressing electron-hole recombination and thereby promoting the photodegradation process [11]. Meanwhile, nitrogen doping modifies the electronic structure of TiO_2, enabling more effective separation of photogenerated electrons and holes. This increases the availability of charge carriers for surface reactions, including the formation of hydroxyl radicals. Nitrogen also influences the surface characteristics of TiO_2, enhancing the adsorption of reactant molecules and strengthening interactions between the photocatalyst and target pollutants [32].

Hence, the presence of dual dopants effectively narrows the band gap, thereby improving the material's ability to absorb visible light. Additionally, the recombination of electron-hole pairs is more effectively suppressed, as the electrons are captured by both Cu and nitrogen dopants. Furthermore, the optimization of calcination temperature for co-doping photocatalysts also influences the photodegradation efficiency as shown in Figure 8(b). It is evident that escalating the calcination temperature initially enhances photocatalytic performance [17]. However, at elevated temperatures, the improvement becomes less pronounced. This trend can be attributed to changes in both crystallinity and Eg.

As the calcination temperature increases, the crystallinity of the material improves. Typically, higher crystallinity is associated with reduced surface adsorption capacity, which can negatively

impact photocatalytic degradation. However, the data from this study suggest a contrasting behaviour, indicating that the influence of crystallinity on photocatalytic activity is relatively minor. With increasing calcination temperature, the band gap energy tends to decrease, enhancing the material's ability to absorb visible light. This improved light absorption promotes the generation of •OH radicals, which are essential for the degradation of organic pollutants. It is important to note that a smaller Eg facilitates stronger visible-light absorption and more efficient radical formation, thereby improving photocatalytic degradation. Conversely, a larger Eg limits light absorption and reduces photocatalytic efficiency [14]. Within the studied temperature range, it is clear that Eg plays a more dominant role than crystallinity in determining the photocatalytic performance of TiO_2 [27]. Nevertheless, when the temperature rises above 500 °C, accompanied by an increase in crystallinity, the reduction in Eg becomes less pronounced, leading to a relatively larger band gap. Under these conditions, the decline in photocatalytic efficiency is likely governed by both the relatively large grain size and the high degree of crystallinity.

3.2.3. The Effect of Photocatalyst Mass

As shown in Figure 9(a), an increase in photocatalyst mass clearly enhances the photocatalytic degradation efficiency. However, this trend reverses when an excessive amount of photocatalyst is used. A higher photocatalyst dosage provides more active surface area and generates a greater number of •OH radicals, thereby improving the degradation process. Nevertheless, excessive photocatalyst loading can increase the turbidity of the solution, which obstructs light penetration. This reduction in light availability limits the formation of •OH radicals and ultimately diminishes the overall photocatalytic efficiency. Based on the obtained data, it is evident that 100 mg is the optimal photocatalyst dosage for the degradation of 100 mL of AMX solution.

3.2.4. The Effect of Solution pH

Figure 9(b) illustrates the effect of solution pH on the photocatalytic degradation efficiency of AMX. It is noted in Figure 9 that the degradation proceeds slowly at very low pH levels, which only attained a maximum point at around 20% in 150 min. Then, it increases progressively until reaching approximately 90% with rising pH, but begins to decline to nearly 70% at pH values above 6. The lowest photocatalytic degradation efficiency observed at pH 2 can be attributed to the positive charge present on both the TiO_2-Cu/N photocatalyst surface and the AMX molecules [5][20]. This similarity in charge leads to electrostatic repulsion, which hinders the adsorption of AMX onto the photocatalyst surface, thereby reducing its degradation efficiency. At pH 4, the photocatalyst surface becomes largely uncharged, while the positive charge on AMX molecules diminishes.

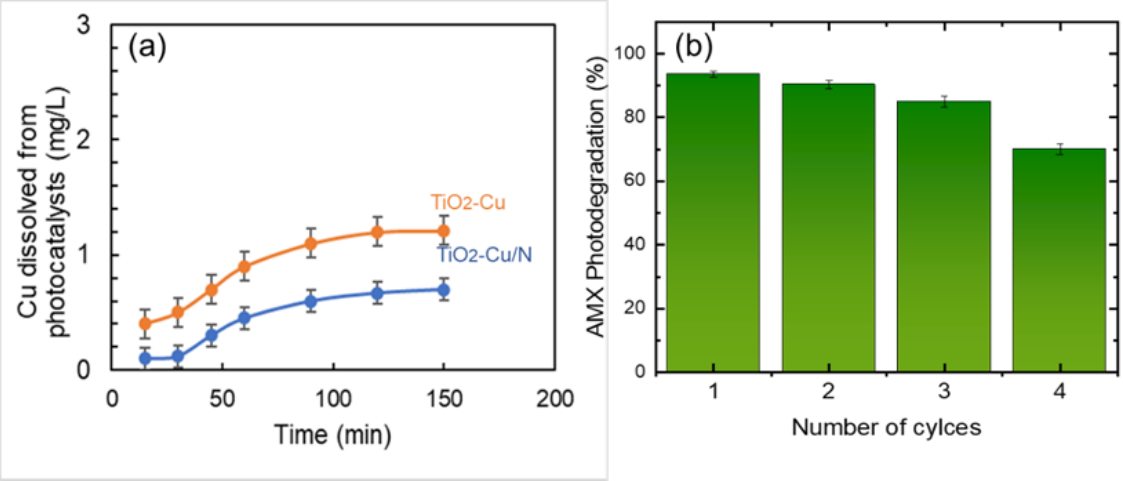

Figure 10. The effect of N doping on (a), copper incorporation and (b) the recyclability of the photocatalyst.

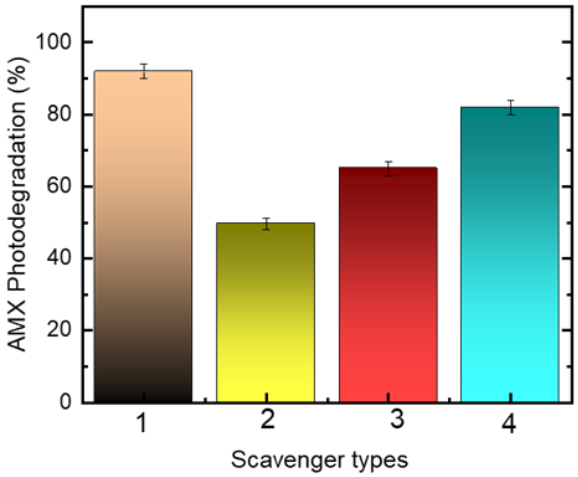

Figure 11. Effect of the radical scavenger agents: (1) No agent, (2) iso-propanol, (3) $(NH_4)_2C_2O_4$, and (4) Na_2-EDTA.

This condition allows for more favourable interactions between the photocatalyst and the pollutant, contributing to the improved degradation efficiency observed at this pH.

At pH 6, the photocatalyst surface begins to acquire a slight negative charge, although it remains predominantly neutral (TiOH), while amoxicillin exists mainly in a zwitterionic form. This charge balance facilitates effective mutual interaction. Additionally, the neutral surface of TiO_2-Cu/N promotes the formation of •OH radicals, and the increased presence of surface –OH groups enhances radical generation. The resulting higher concentration of •OH radicals leads to more efficient photocatalytic degradation. At pH 8, both the TiO_2-Cu/N surface and the AMX molecules carry negative charges, resulting in electrostatic repulsion that inhibits the adsorption of AMX onto the photocatalyst. Consequently, the degradation efficiency decreases under these alkaline conditions. This finding confirms that pH 6 is the optimal condition for the degradation of 100 mL of AMX solution.

3.2.5. The Effect of the Reaction Time

The effectiveness of AMX photodegradation under visible light irradiation using the TiO_2-Cu/N photocatalyst over varying reaction times is also presented in Figure 9. Under prolonged visible light irradiation, the photocatalytic degradation becomes increasingly effective from around 20% in 15 minutes initial time photodegradation process to nearly 90% using a maximum photocatalyst dose of 150 mg. It can occur due to enhanced interaction between the light and the photocatalyst, leading to a greater generation of •OH radicals. In this condition, the contact between AMX molecules and the •OH radicals also becomes more efficient, thereby promoting more effective degradation. Over -extended reaction times, the photocatalytic degradation activity of TiO_2-Cu/N tends not to increase and may even decline due to several factors. One key reason is the possible saturation of active sites on the catalyst surface, which limits further degradation once most of the pollutant molecules have been broken down. Additionally, prolonged exposure to light can lead to photocorrosion or structural changes in the TiO_2-Cu/N catalyst, reducing its effectiveness. Another contributing factor is the accumulation of intermediate products or by-products on the catalyst surface, which can block active sites and hinder light absorption, thereby suppressing further photocatalytic activity. The presented data conclude that 2 h is the optimal duration for the degradation process

3.2.6. The Effect of N Doping on Copper Incorporation and the Recyclability of the Photocatalyst

The stability of the photocatalyst was evaluated based on the amount of copper leached during the

photocatalytic degradation process under optimal conditions, as presented in Figure 10. The data notifies that copper dissolution from the doped photocatalyst was very low, with concentrations remaining below 1 mg/L throughout the degradation process. Copper leaching increased slightly with prolonged reaction time. Notably, the N–Cu co-doped TiO_2 exhibited lower copper dissolution compared to the single Cu-doped TiO_2, suggesting that nitrogen co-doping enhances the stability of copper dopants by suppressing their leaching.

Furthermore, the photocatalyst maintained its activity over 3 consecutive degradation cycles, but forth repeating the performace decreases as small as nearly 20% reduction. It is also demonstrated in Figure 10, confirming its good reusability and structural integrity. Meanwhile, the relatively small reduction of AMX photodegradation from 90% to 70% may cause by fouling activity onto photocatalyst surface, releasing of Cu dopant, and alteration of crystal sructure which is reduces the active sites and triggers the electron-hole combination. Those all effect may contribute to lowering the photocatalyst performance as well as AMX photodegradation efficiency [33][34].

3.2.7. The Effect of the Addition of the Radical Scavenger Agents

During the photocatalytic process, h^+ (hole: positive radical), •OH radicals, and superoxide radicals ($•O_2^-$) are formed, as illustrated by equations (1-5) [20][21], and play a vital role in the photodegradation of organic compounds, including AMX. To identify the predominant reactive species involved in the degradation, a scavenger agent test was performed, with the results presented in Figure 11. The scavenger agents employed were $(NH_4)_2C_2O_4$, isopropanol, and Na_2-EDTA, which selectively quench $•O_2^-$, •OH, and h^+, respectively. The data reveal that the most significant decrease in AMX degradation efficiency occurred in the presence of isopropanol, followed by $(NH_4)_2C_2O_4$, and then Na_2-EDTA. These findings indicate that •OH radicals are the primary species responsible for the degradation of the organic pollutant, with $•O_2^-$ radicals contributing to a lesser extent, and photogenerated holes playing a comparatively minor role.

4. CONCLUSIONS

This study demonstrates the successful synthesis of a visible-light-responsive TiO_2-Cu/N photocatalyst using copper sourced from electroplating wastewater and nitrogen co-doping via a sol–gel method. Characterization results confirmed that optimal doping levels—0.65% Cu and 30% N—combined with optimum calcination temperature at 500 °C, produced a stable anatase phase with significantly narrowed bandgap and elevated photocatalytic performance for AMX degradation under visible light. Moreover, nitrogen co-doping effectively stabilized the Cu dopant within the TiO_2-Cu/N matrix, enabling the photocatalyst to maintain high performance over three consecutive degradation cycles without notable loss of activity. The highest degradation efficiency was achieved under mild conditions (pH 6, 2 h irradiation, 100 mg photocatalyst) as much as 90% with hydroxyl radicals identified as the primary reactive species. Overall, this work highlights a sustainable and effective approach to photocatalyst development, leveraging industrial waste as a dopant source for advanced water treatment applications.

AUTHOR INFORMATION

Corresponding Author

Endang Tri Wahyuni — Chemistry Department, Gadjah Mada University, Yogyakarta-55281 (Indonesia);
orcid.org/0000-0002-0584-0549
Email: endang_triw@ugm.ac.id

Authors

Kusuma Putri Suwondo — Research Center for Advanced Materials, National Research and Innovation Agency (BRIN), Banten-14314 (Indonesia);
orcid.org/0000-0002-4343-1009

Nurul Hidayat Aprilita — Chemistry Department, Gadjah Mada University, Yogyakarta-55281 (Indonesia);
orcid.org/0000-0002-2132-6646

Nur Farhana Jafaar — School of Chemical Sciences, Universiti Sains Malaysia (USM), Pulau Pinang-11800 (Malaysia);

orcid.org/0000-0001-6529-1337
Early Zahwa Alharissa — Research Center for Nanoscience and Nanotechnology, Institut Teknologi Bandung, Bandung-40132 (Indonesia);
orcid.org/0009-0007-8960-2866

Author Contributions

Conceptualization, and writing original draft, E. T. W., K. P. S; Writing– review & editing, E. Z. A.; Visualization, K. P. S., E. Z. A.; Investigation, K. P. S.; Methodology, E. T. W., K. P. S., E. Z. A.; Supervision and Validation, E. T. W., N. H. A., N. F. J.

Conflicts of Interest

The authors declare no conflict of interest.

ACKNOWLEDGEMENT

The authors would like to express sincere gratitude and appreciation to Universitas Gadjah Mada (UGM) and the Indonesia Endowment Fund for Education (LPDP) for their generous support through the Post-Doctoral Research Grant with Contract Number: 4292/UN1.P1/PT.01.03/2024, 5 April 2024.

DECLARATION OF GENERATIVE AI

During the preparation of this work, the authors used ChatGPT (OpenAI) to enhance the clarity and readability of the manuscript. After using this tool, the authors thoroughly reviewed and edited the content and take full responsibility for the final version of the publication.

REFERENCES

[1] S. A. Ansari, M. M. Khan, M. O. Ansari, and M. H. Cho. (2016). "Nitrogen-Doped Titanium Dioxide (N-Doped TiO2) for Visible Light Photocatalysis". *New Journal of Chemistry.* **40** : 3000-3009. 10.1039/C5NJ03478G.

[2] C. Byrne, R. Fagan, S. Hinder, D. E. McCormack, and J. A. Byrne. (2016). "New Approach to Modifying the Anatase-to-Rutile Transition Temperature in Titanium Dioxide Photocatalysts". *RSC Advances.* **6** : 95232-95238. 10.1039/C6RA19759K.

[3] D. Balarak, N. Mengelizadeh, P. Rajiv, and K. Chandrika. (2021). "Photocatalytic Degradation of Amoxicillin from Aqueous Solutions by Titanium Dioxide Nanoparticles Loaded on Graphene Oxide". *Environmental Science and Pollution Research.* **28** : 49743-49754. 10.1007/s11356-021-13525-1.

[4] X. Bian, Y. Xia, T. Zhan, L. Wang, W. Zhou, Q. Dai, and J. Chen. (2019). "Electrochemical Removal of Amoxicillin Using a Copper-Doped Lead Dioxide Electrode: Electrode Characterization, Operational Parameters Optimization, and Degradation Mechanism". *Chemosphere.* **233** : 762-770. 10.1016/j.chemosphere.2019.05.226.

[5] S. Chandra, P. Jagdale, I. Medha, A. K. Tiwari, M. Bartoli, A. Nino, and F. Olivito. (2021). "Biochar-Supported Titanium Dioxide-Based Nanocomposites for the Photocatalytic Degradation of Sulfamethoxazole in Water: A Review". *Toxics.* **9** (11): 313. 10.3390/toxics9110313.

[6] A. Din, S. B. Khan, M. I. Khan, S. A. Asif, M. A. Khan, S. Gul, K. Akhtar, and A. M. Asiri. (2017). "Cadmium Oxide-Based Efficient Electrocatalyst for Hydrogen Peroxide Sensing and Water Oxidation". *Journal of Materials Science: Materials in Electronics.* **28** : 19017-19024. 10.1007/s10854-016-5633-8.

[7] A. Hajjaji, S. Jemai, A. Rebhi, K. Trabelsi, M. Gaidi, A. N. Alhazaa, M. A. Al-Gawati, M. A. El Khakani, and B. Bessais. (2020). "Enhancement of Photocatalytic and Photoelectrochemical Properties of Titanium Dioxide Nanotubes Sensitized by SILAR-Deposited Lead Sulfide Nanoparticles". *Journal of Materials.* **6** (1): 62-69. 10.1016/j.jmat.2019.12.002.

[8] L. Hua, Z. Yin, and S. Cao. (2020). "Recent Advances in the Synthesis and Applications of Carbon-Doped Titanium Dioxide Nanomaterials". *Catalysts.* **10** : 143. 10.3390/catal10121431.

[9] P. Karuppasamy, N. R. N. Nisha, A. Pugazhendhi, S. Kandasamy, and S.

Pitchaimuthu. (2021). "Transition Metal (Zn, Zr, Cu)-Doped Titanium Dioxide Photocatalysts for Enhanced Photocatalytic Decoloration of Methylene Blue under Visible Light Irradiation". *Journal of Environmental Chemical Engineering.* **9** (4): 105254. 10.1016/j.jece.2021.105254.

[10] S. Khan, T. L. Ruwer, N. Khan, A. Köche, R. W. Lodge, H. Coelho-Júnior, R. L. Sommer, M. J. L. Santos, C. F. Malfatti, C. P. Bergmann, and J. A. Fernandes. (2021). "Revealing the Impact of Interstitial and Substitutional Nitrogen Doping in Titanium Dioxide on Photoelectrochemical Applications". *Journal of Materials Chemistry A.* **9** : 12214-12224. 10.1039/D0TA11494D.

[11] H. Lee, H. S. Jang, N. Y. Kim, and J. B. Joo. (2021). "Copper-Doped Titanium Dioxide Hollow Nanostructures for Enhanced Photocatalysis under Visible Light Conditions". *Journal of Industrial and Engineering Chemistry.* **99** : 352-363. 10.1016/j.jiec.2021.04.045.

[12] Q. Li, R. Jia, J. Shao, and Y. He. (2019). "Photocatalytic Degradation of Amoxicillin via Titanium Dioxide Nanoparticles Coupled with a Submerged Porous Ceramic Membrane Reactor". *Journal of Cleaner Production.* **209** : 755-761. 10.1016/j.jclepro.2018.10.183.

[13] S. S. Malik and S. Mundra. (2023). "Increasing Consumption of Antibiotics during the COVID-19 Pandemic: Implications for Patient Health and Emerging Antimicrobial Resistance". *Antibiotics.* **12** (1): 45. 10.3390/antibiotics12010045.

[14] M. Pelaez, N. T. Nolan, S. C. Pillai, M. K. Seery, P. Falaras, A. G. Kontos, P. S. M. Dunlop, J. W. J. Hamilton, J. A. Byrne, K. O'Shea, M. H. Entezari, and D. D. Dionysiou. (2012). "Visible-Light-Active Titanium Dioxide Photocatalysts for Environmental Applications: A Review". *Applied Catalysis B: Environmental.* **125** : 331-349. 10.1016/j.apcatb.2012.05.036.

[15] A. Piątkowska, M. Janus, K. Szymański, and S. Mozia. (2021). "Carbon-, Nitrogen-, and Sulfur-Doped Titanium Dioxide Photocatalysts: A Review". *Catalysts.* **11** (1): 144. 10.3390/catal11010144.

[16] A. Rafiq, M. Ikram, S. Ali, F. Niaz, M. Khand, Q. Khan, and M. Maqbool. (2021). "Photocatalytic Degradation of Dyes Using Semiconductor Photocatalysts to Clean Industrial Water Pollution". *Journal of Industrial and Engineering Chemistry.* **97** : 111-128. 10.1016/j.jiec.2021.02.017.

[17] S. M. Reda, M. Khairy, and M. A. Mousa. (2020). "Photocatalytic Activity of Nitrogen- and Copper-Doped Titanium Dioxide Nanoparticles Prepared by Microwave-Assisted Sol–Gel Process". *Arabian Journal of Chemistry.* **13** (1): 86-95. 10.1016/j.arabjc.2017.02.002.

[18] S. Rodriguez-Mozaz, S. Chamorro, E. Martí, B. Huerta, M. Gros, A. Sánchez-Melsió, C. M. Borrego, D. Barceló, and J. L. Balcázar. (2015). "Occurrence of Antibiotics and Antibiotic Resistance Genes in Hospital and Urban Wastewaters and Their Impact on the Receiving River". *Water Research.* **69** : 234-242. 10.1016/j.watres.2014.11.021.

[19] S. Shen, T. Ke, D. Fang, and D. Lin. (2022). "Nitrogen and Sulfur Co-Doping of TiO2@C Derived from In Situ Oxidation of Ti3C2 MXene for Efficient Persulfate Activation and Sulfamethoxazole Degradation under Visible Light". *Separation and Purification Technology.* **297** : 121460. 10.1016/j.seppur.2022.121460.

[20] K. P. Suwondo, E. Z. Alharissa, N. H. Aprilita, and E. T. Wahyuni. (2025). "Remarkable Enhancement of Nitrogen-Doped Titanium Dioxide Activity under Visible Light by Codoping with Copper from Electroplating Wastewater for Degradation of Amoxicillin Residual in Water Media". *ACS Omega.* **10** : 7722-7733. 10.1021/acsomega.4c07853.

[21] K. P. Suwondo, N. H. Aprilita, and E. T. Wahyuni. (2022). "Enhancement of Titanium Dioxide Photocatalytic Activity under Visible Light by Doping with Copper from Electroplating Wastewater". *Reaction Kinetics, Mechanisms and Catalysis.* **135** : 479-497. 10.1007/s11144-021-02134-1.

[22] T. Tatarchuk, N. Danyliuk, A. Shyichuk, W. Macyk, and M. Naushad. (2021). "Photocatalytic Degradation of Dyes Using Rutile Titanium Dioxide Synthesized by Reverse Micelle and Low-Temperature Methods: Real-Time Monitoring of Degradation Kinetics". *Journal of Molecular Liquids.* **342** : 117407. 10.1016/j.molliq.2021.117407.

[23] C. Thambiliyagodage and L. Usgodaarachchi. (2021). "Photocatalytic Activity of Nitrogen-, Iron-, and Copper-Co-Doped Titanium Dioxide Nanoparticles under Sunlight". *Current Research in Green and Sustainable Chemistry.* **4** : 100186. 10.1016/j.crgsc.2021.100186.

[24] B. Thirupathi and P. G. Smirniotis. (2011). "Co-Doping of Metals on Mn/TiO2 Catalysts and Its Effect on the Selective Reduction of NO with NH3 at Low Temperatures". *Applied Catalysis B: Environmental.* **110** : 195-206. 10.1016/j.apcatb.2011.09.001.

[25] N. Türkten, Z. Cinar, A. Tomruk, and M. Bekbolet. (2019). "Copper-Doped Titanium Dioxide Photocatalysts: Application to Drinking Water by Humic Matter Degradation". *Environmental Science and Pollution Research.* **26** : 36096-36106. 10.1007/s11356-019-04474-x.

[26] D. Vaya and P. K. Surolia. (2020). "Semiconductor-Based Photocatalytic Degradation of Pesticides: An Overview". *Environmental Technology & Innovation.* **20** : 101128. 10.1016/j.eti.2020.101128.

[27] E. T. Wahyuni, P. Y. Yulikayani, and N. H. Aprilita. (2020). "Enhancement of Visible-Light Photocatalytic Activity of Copper-Doped Titanium Dioxide for Photodegradation of Amoxicillin in Water". *Journal of Materials and Environmental Science.* **11** (4): 670-683.

[28] S. Wu, H. Hu, Y. Lin, J. Zhang, and Y. H. Hu. (2020). "Visible-Light Photocatalytic Degradation of Tetracycline over Titanium Dioxide". *Chemical Engineering Journal.* **382** : 122842. 10.1016/j.cej.2019.122842.

[29] X. Yang, Z. Chen, W. Zhao, C. Liu, X. Qian, M. Zhang, G. Wei, E. Khan, Y. H. Ng, and Y. S. Ok. (2021). "Recent Advances in Photodegradation of Antibiotic Residues in Water: A Review". *Chemical Engineering Journal.* **405** : 126806. 10.1016/j.cej.2020.126806.

[30] Q. Yuan, Y. Li, and G. Yin. (2019). "Synthesis of Carbon- and Nitrogen-Codoped Titanium Dioxide Hollow Spheres by a Dual-Frequency Atmospheric Pressure Cold Plasma Jet". *Journal of Materials Science.* **54** : 12488-12497. 10.1007/s10853-019-03804-1.

[31] H. C. Yilmaz, E. Akgeyik, S. Bougarrani, M. El Azzouzi, and S. Erdemoglu. (2020). "Photocatalytic Degradation of Amoxicillin Using Co-Doped TiO2 Synthesized by Reflux Method and Monitoring of Degradation Products by LC–MS/MS". *Journal of Dispersion Science and Technology.* **41** (3): 414-425. 10.1080/01932691.2019.1583576.

[32] D. Zhang, J. Chen, Q. Xiang, Y. Li, M. Liu, and Y. Liao. (2019). "Transition-Metal-Ion (Cr, Co, Cu, Fe, Mn) Doping of TiO2 Nanotubes: A General Approach". *Inorganic Chemistry.* **58** (19): 12511-12515. 10.1021/acs.inorgchem.9b01889.

[33] Y. Tai, B. Yang, J. Li, L. Meng, P. Xing, and S. Wang. (2024). "Design and Preparation of Heterostructured Cu2O/TiO2 Materials for Photocatalytic Applications". *Molecules.* **29** (21): 5028. 10.3390/molecules29215028.

[34] P. Nazari, S. Sohrabi, F. Akhlaghian, M. Mansouri, and M. M. Mohammadi. (2024). "Activity, Stability, and Kinetic Study of CuO/TiO2 Janus Photocatalyst for Rhodamine B Degradation". *Water Practice and Technology.* **19** (5): 1893-1907. 10.2166/wpt.2024.118.